Inorganic Chemistry

Article

pubs.acs.org/IC

Tailoring Nanoscale Friction in MX_2 Transition Metal Dichalcogenides

Antonio Cammarata*[,†] and Tomáš Polcar[†,‡]

[†]Department of Control Engineering, Czech Technical University in Prague, Technicka 2, 16627 Prague 6, Czech Republic

[‡]Engineering Materials & nCATS, FEE, University of Southampton, SO17 1BJ Southampton, United Kingdom

Supporting Information

ABSTRACT: Lattice dynamics of MX_2 transition metal dichalcogenides (M = Mo, W; X = S, Se, Te) have been studied with density functional theory techniques to control the macroscopic tribological behavior. Long-range van der Waals forces have been modeled with Grimme correction to capture the interlayer interactions. A new lattice dynamic metric, named *cophonicity*, is proposed and used in combination with electronic and geometric descriptors to relate the stability of the lattice distortions with the electro-structural features of the system. The cophonicity analysis shows that the distortion modes relevant to the microscopic friction can be controlled by tuning the relative M/X atomic contributions to the phonon density of states. Guidelines on how to engineer macroscopic friction at nanoscale are formulated, and finally applied to design a new Ti-doped MoS_2 phase with enhanced tribologic properties.

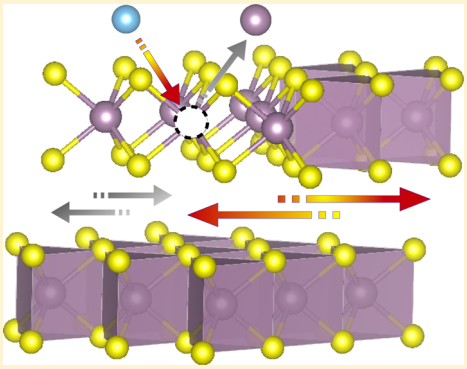

INTRODUCTION

The control of friction by lubricants is a great issue in automotive or aerospace industrial applications, that strongly addresses research efforts toward the comprehension of the mechanisms underlying friction, wear, and lubrication.[1,2] Great attention has been directed to transition metal dichalcogenides (TMDs) because of their close features with graphene and their highly versatile chemical composition.[3] They find tribologic applications in all those situations in which liquid lubricants cannot be used, such as in a vacuum, in extreme-temperature conditions, or for facile expulsion from the gaps between moving parts in a device.

Numerous studies have been devoted mainly to the electronic properties,[4−6] while only a few theoretical papers have dealt with the tribologic aspects;[7−11] most of them have been devoted solely to the study of the MoS_2 compound. The atomic description of friction is usually provided in terms of the atom arrangement forming the sliding surfaces and the lubricant in between them; Newtonian (or Langevin) equations of motion are solved in the presence of an external load and a drift force pulling the sliding surfaces. In this way, it is possible to sample the evolution of the geometry of the system in order to obtain information on friction, adhesion, and wear.[2] This represents a standard example of how MD simulations are used to model the tribological properties at the atomic scale; despite their capability to simulate thousand-atom systems, their results can hardly be transferred across the stoichiometries, since they rely on force fields designed *ad hoc* for the studied system. Moreover, a deeper insight of the local electronic and geometric characteristics is required to capture subtleties that a molecular mechanic description cannot represent; indeed, quantum mechanical approaches have been used to this aim,[12] focusing on the theoretical modeling of a specific stoichiometry and chemical composition.

The selection of the proper chemical composition, stoichiometry, and geometry to obtain a TMD compound with reduced friction coefficient has been, so far, based mainly on experimental data, while theoretical works have had the role to model the selected material to uncover peculiar properties. A broader theoretical framework encompassing all the compounds of the TMD family would help researchers to focus the experimental exploration on only those materials that are promising candidates with enhanced frictional properties. However, to the best of our knowledge, a unified description of the electronic and structural features common to all the MX_2 compounds and relevant to the tribological properties is missing at the quantum mechanical level. In the present work, our goal is to identify how the electronic and structural features of MX_2 TMDs determine the macroscopic friction, in order to engineer the tribological properties at the atomic scale. Using density functional theory based techniques, we formulate a new lattice dynamics descriptor, that we denote as *cophonicity*, based on the dynamic properties of the M and X atomic species; with such a descriptor, we are able to disentangle the atomic electro-structural contributions to the lattice vibrations affecting the layer sliding. Our approach enables us to capture the electronic and geometric features that are common to the MX_2 TMDs systems and responsible for the frictional properties; in this way, we formulate a protocol to properly choose and modify the MX_2 stoichiometry, geometry, and chemical composition to obtain TMD compounds with improved frictional response. Finally, we apply such a protocol to suggest a particular Ti-

Received: February 22, 2015
Published: May 22, 2015

DOI: 10.1021/acs.inorgchem.5b00431
Inorg. Chem. 2015, 54, 5739−5744

doped MoS_2 phase as new material with enhanced tribologic characteristics.

COMPUTATIONAL DETAILS

MX_2 transition metal dichalcogenides are layered structures, with each layer formed by hexagonally packed metal atoms (M) forming covalent bonds with six chalcogen anions (X) in a trigonal prismatic cordination (Figure 1); adjacent layers are coupled by weak van der Waals forces that allow relative sliding under tribological conditions. Several stable TMD polymorphs and polytypes are found,[3] with some transforming into each other by sliding of subsequent layers; such sliding motions include also rotations (reorientations) of one layer with respect to its two adjacent ones about an orthogonal axis. The complex atomic displacements that result into layer sliding, either commensurate or not, can be represented as linear combinations of collective atomic motions, e.g., phonon or vibrational modes, of two adjacent layers of the most stable configuration. We will thus focus on model systems with two layers in the unit cell, and we choose 2H polymorph crystalline MX_2 structures as model geometries, with M = Mo, W and X = S, Se, Te, and hexagonal $P6_3/mmc$ symmetry (SG 194); for simplicity, we will refer to them as MX by dropping the stoichiometric coefficients. We choose the 2H configuration in which two adjacent layers are oriented in such a way that an M atom of one layer is aligned with two X atoms of the other one along the direction orthogonal to each layer (*c*-axis in our setting, see Figure 1); this choice is motivated by a recent ab initio study on the MoS_2 compound,[12] where it has been shown that this configuration corresponds to the lowest energy value found for several arrangements of two subsequent MoS_2 layers.

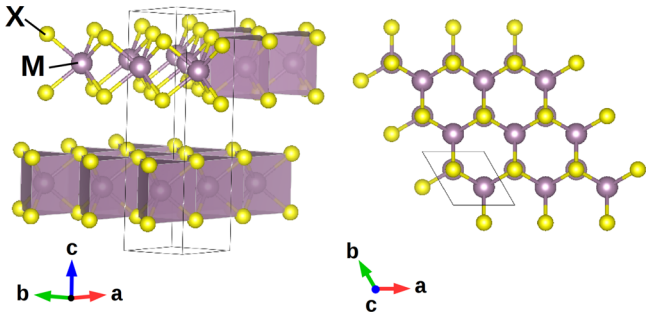

Figure 1. Hexagonal $P6_3/mmc$ structure of 2H polymorph MX_2 model geometries (M = transition metal, X = chalcogen atom). M−X bonds are arranged in a trigonal prismatic coordination forming MX_2 layers that can slide thanks to weak van der Waals interactions.

Our density functional theory (DFT) calculations are performed using the projector-augmented wave (PAW) formalism and the Perdew−Burke−Ernzerhof (PBE) energy functional[13] with van der Waals correction as implemented in the most recent version of VASP[14] package. Particular attention has been paid to the choice of the description of the van der Waals interactions, that are known to play an important role in determining the static and dynamic properties of TMDs;[15] after preliminary benchmarks, we chose the Grimme correction,[16] that is able to capture the structural features. The Brillouin zone is sampled with a minimum of a 5 × 5 × 3 *k*-point mesh and plane wave cutoff of 550 eV. Full structural (atoms and lattice) relaxations are initiated from diffraction data[17−22] and the forces minimized to a 0.5 meV $Å^{-1}$ tolerance. We computed the phonon band structure of each considered system using the fully relaxed geometries, aided by the PHONOPY software.[23]

RESULTS AND DISCUSSION

The goal of our study is to identify and control the bulk features that contribute to the macroscopic friction. To this aim, we start with the characterization of the atomic motions that produce a global slide of adjacent layers. All the possible sliding directions can be represented as suitable linear combinations of vibrational modes; for this reason, no assumption is done on the layer drift, and our conclusions will be valid irrespective of the sliding direction. To investigate the electron−lattice effect on the macroscopic tribological properties, we need first to identify the phonon modes directly related to the sliding of adjacent layers. We thus compute each phonon band structure (Figure 2) along a linear path joining the high-symmetry points of the irreducible Brillouin zone (IBZ); we do not find any unstable displacements, confirming that the considered geometries represent stable configurations. We then characterize each vibrational mode at a fixed *k*-point by analyzing the corresponding atomic displacements. Since all six compounds have the same geometry and the same set of structural symmetries, they share the same set of vibrational modes, with frequencies depending only on the atomic types. We observe that a variation of the atomic species produces a shift of the vibrational frequencies and a variation of the M/X relative contribution (pDOS in Figure 2) to the vibrational bands.

Only a few modes are related to sliding motion, corresponding to pure rigid layer translations or to layer shifts combined with intralayer motions, like stretching and/or bending of atomic bonds or flattening of coordination polyhedra (top of Figure 2). Our goal is to lower the frequency of those vibrational modes that are relevant to the layer sliding, in order to facilitate those kinds of atomic displacements that correspond to a global shift of one layer with respect to its two adjacent ones. This can be understood in terms of the classical picture, where the frequency represents the curvature of the system energy hypersurface as a function of the atomic coordinates. In modeling tribological conditions, at the working regime of the tribological material, the system energy can be considered as constant; at fixed system energy, the lower the frequency of a mode is, the higher the amplitude of the corresponding atomic displacement is. Concerning the phonon modes that are associated with the layer sliding, a higher amplitude of the atomic displacements corresponds to an enhanced shift of one layer with respect to its adjacent ones, hence favoring the sliding of the layers.

The frequencies of the sliding-related modes are found to be highest for MoS_2 and lowest for WTe_2, following the ordering MoS_2 > $MoTe_2$ > $MoSe_2$ > WS_2 > WSe_2 > WTe_2; such ordering is expected to be the same for the bulk contribution to the macroscopic friction coefficients of the corresponding materials. It is worth noting here that a direct comparison with available experimental data is not straightforward, since this is not fully comparable due to the different experimental conditions.[24−30] Moreover, our models are aimed at studying the resistance of layer shearing in the bulk of the structure, while experimentally measured macroscopic friction is almost inevitably related also to wear and surface effects due to exfoliation, absorption of small molecules, presence of oxidizing agents, and elastic effects related to the number of layers.[24]

In order to quantify how the chemical composition determines the mode frequency, we need to relate the electronic and geometric properties of the structure to the frequency shift. We recall that the vibrational frequencies of the lattice are determined by the atomic types involved in the formation of the structure, their geometric arrangement, and the symmetries that the latter determines. Once the atomic topology (atom coordination shells) is fixed, the kinds of

DOI: 10.1021/acs.inorgchem.5b00431
Inorg. Chem. 2015, 54, 5739−5744

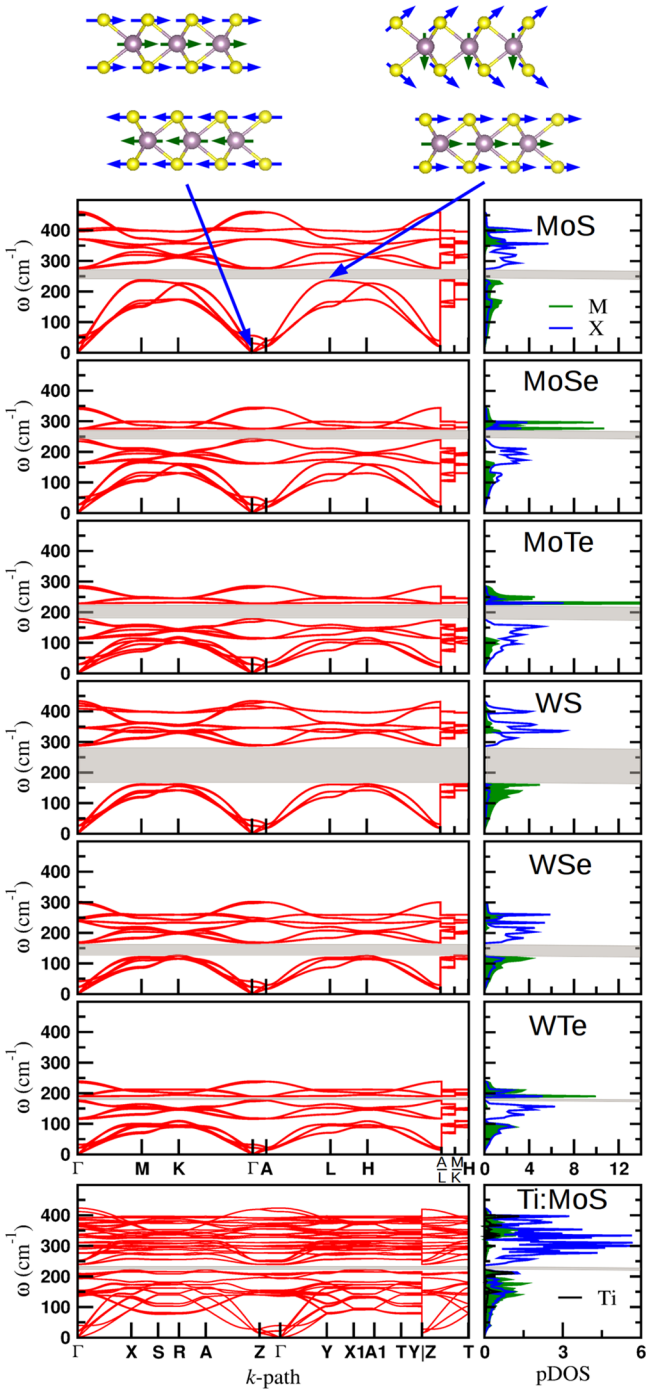

Figure 2. Computed phonon band structures (left panels) and phonon-DOS (right panels) of MX_2 compounds; the gray area in each plot indicates the energy gap separating the low- from the high-frequency band. In the inset, examples of vibrational modes relevant to the macroscopic friction are shown: pure layer sliding (top left) and layer sliding combined with intralayer asymmetric M−X−M bond stretching (top right).

atomic displacements, that is, the vibrational modes, and hence the corresponding phonon band structure, are determined. A specific vibrational mode is the result of the colletive motion of ions of distinct atomic type; each ion contributes to the collective motion in an amount that depends on the electronic structure of the environment where it is embedded that, in turn, depends on the electronic characteristics of the nearest neighboring atoms. For this reason, at a fixed topology, the atomic type determines the vibrational frequency of the modes.

To disentangle the electronic from the structural contributions to the determination of the phonon frequencies, we first quantify the geometric distortions δ[31] of the system by performing a group-theoretical analysis with the aid of the ISODISTORT software;[32] we thus decompose the MX geometries in terms of distortions of a parent phase, that we choose to be the relaxed MoS structure (Table 1). We then evaluate the M−X bond covalency $C_{M,X}$ at different structural distortions, applying the covalency metric (see Supporting Information), designed for crystalline materials,[33] in the energy range of the valence band. The $C_{M,X}$ bond covalency is a measure of the electronic density distributed along the M−X bond; it is determined by the cooperative effect of the electronic structure of the M and X atoms and the structural distortions of the system, as has been already observed in a theoretical study on perovskite oxides.[33] We observe that covalency is strictly decreasing with distortions in MoX systems, while it has a minimum for the WTe compounds among the WX compositions (Table 1 and Figure 3a).

We now need a metric to quantify how changing the atomic type affects specific vibration frequencies. Each phonon mode is a complex function of all the components of the force constant tensors of all the atomic pairs present in the system;[34] a particular displacement pattern, including those representing the layer sliding, cannot be related to single components of the force constant tensors in a unique way. Therefore, the force constants alone do not represent a manageable descriptor to parametrize the interactions responsible of specific atomic displacements, the layer sliding among them. To obtain a simple metric, we focus on the smallest unit that produces the dynamical interactions, that is, the M−X atomic pair. We call this metric *cophonicity of the M-X atomic pair* C_{ph}(M−X), and we use it as a lattice dynamics descriptor to understand the atomic type dependence of phonon frequencies. The complete mathematical implementation is described in the Supporting Information together with a discussion on its validity and limitations.

We thus use the cophonicity metric to relate the vibrational frequency to the atomic types that generate the corresponding distortion mode. All the computed pDOSs show two distinct energy bands, corresponding to low- and high-frenquency ranges, respectively, sparated by a gap. Following the usual convention, we label phonon bands with progressive integer numbers, starting from the lowest associated frequency. With this convention, $\Gamma(1)$ represents the vibrational mode associated with band number 1, that is, the displacive mode associated with the lowest frequency $\omega(\Gamma)_1$ at the Γ point of the IBZ; analogously, $\Gamma(2)$ is associated with the vibrational mode with frequency $\omega(\Gamma)_2$ such that $\omega(\Gamma)_3 \geq \omega(\Gamma)_2 \geq \omega(\Gamma)_1$ and so on. We analyzed the trend of all the frequencies associated with the sliding-related modes against the cophonicity of the system, and we find that they all have the same trend against the cophonicity metric. For simplicity, in the present analysis, we will discuss only the trend of the degenerate $\omega(\Gamma)_{4-5}$ and $\omega(A)_{1-4}$ frequencies, as our conclusions also apply to the other frequencies that we considered in our study. Irrespective of the kind of phonon mode, we find that the frequency diminishes when C_{ph}(M−X) approaches zero (Table 1 and Figure 3b). If C_{ph} (M−X) = 0, we will say that perfect cophonicity is realized (see Supporting Information).

DOI: 10.1021/acs.inorgchem.5b00431
Inorg. Chem. 2015, 54, 5739−5744

Table 1. Structural Distortion δ (Å), M−X Bond Covalency $C_{M,X}$ (eV), Cophonicity C_{ph}(M−X) (cm^{-1}) of the M−X Pair, Selected Vibrational Frequencies $\omega(k)_i$ (cm^{-1}), and Formation Energy ΔH_f (eV) of the MX_2 Model Systems with MoS System as Reference for Calculating δ and ΔH_f Values

system	δ	$C_{M,X}$	C_{ph}(M−X)	$\omega(\Gamma)_{4-5}$	$\omega(A)_{1-4}$	ΔH_f
MoS	0.00	−0.44	8.3	30	21	0.00
MoSe	0.06	−0.58	−45.7	28	20	2.79
MoTe	0.10	−0.75	−31.0	30	21	5.94
WS	0.02	−0.51	10.0	26	18	1.23
WSe	0.06	−0.66	4.1	24	17	4.27
WTe	0.03	−0.80	0.9	22	15	7.63
Ti:MoS	0.17	−0.76[a]	4.6[b]	$\omega(\Gamma)_4$ 22[c]	$\omega(Z)_{1-2}$ 15[c]	0.04
				$\omega(\Gamma)_5$ 23[c]	$\omega(Z)_{3-4}$ 16[c]	

[a]Ti−S bond covalency value to be compared with $C_{Mo,S}$ in the MoS system. [b]Global cophonicity of Ti:MoS system calculated as weighted average of the C_{ph}(Mo−S) and C_{ph}(Ti−S) cophonicities, with weights corresponding to the M stoichiometric coefficients. [c]Degeneracy of vibrational modes in MoS system is partially lifted in Ti:MoS model, having the latter a lower number of symmetries. According to the displacement patterns, A(1−4) modes of MoS system correspond to Z(1−4) modes of Ti:MoS model.

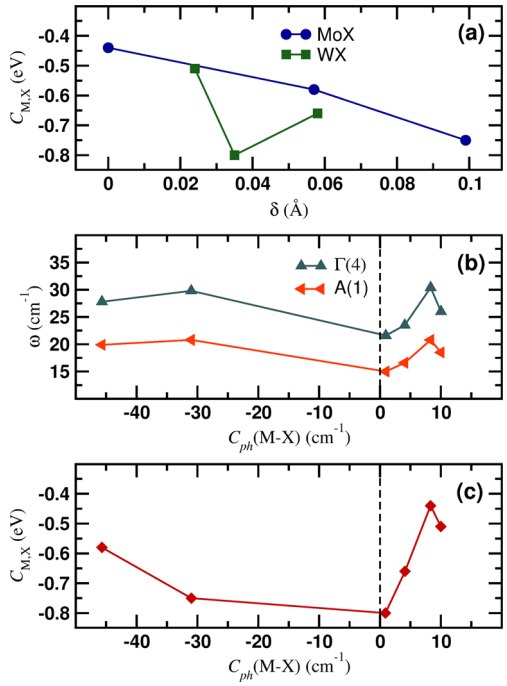

Figure 3. (a) M−X bond covalency as a function of structural distortions δ. Covalency can be tuned by changing the amplitude of the structural distortions. (b) Frequency of the Γ(4) and A(1) modes as a function of M−X pair cophonicity. Irrespective of the vibrational mode, the lowest frequency is realized for C_{ph}(M−X) ≃ 0. (c) Covalency of the M−X bond as a function of C_{ph}(M−X). The lowest $C_{M,X}$ covalency value corresponds to a cophonicity close to zero.

As we discussed above, the $C_{M,X}$ covalency metric captures the entangled electronic and structural features into a single descriptor; thanks to this characteristic, we can relate the change of the phonon frequency to the geometry and the atomic types forming the system by connecting cophonicity with M−X bond covalency. Cophonicity is found to be minimal when $C_{M,X}$ bond covalency is about −0.80 eV, that is realized in the WTe compound (Table 1 and Figure 3c); on the other hand, C_{ph}(M−X) shows similar trends for the MoX and WX compounds with respect to the structural distortions. According to these results, cophonicity, and hence vibrational frequencies, can be adjusted by tuning the distortions and the covalency of the system by a proper selection of the M and X ions.

We now want to exploit the knowledge acquired so far to design a new TMD with enhanced tribological properties. In particular, according to the results discussed above, we want to find an M−X pair that realizes a low covalency value in order to minimize the M−X cophonicity, so as to lower the phonon frequencies that govern the layer drift. We focus on the MoS_2 compound, because the synthesis routes have been extensively studied, and therefore, it constitutes a good candidate to easily grow derived materials. Starting from the MoS model system, we will now design a new compound by partial ion substitution. Among the chosen MoX stoichiometries, MoTe realizes the lowest covalency value; to further lower the Mo−X covalency we must increase the structural distortions (Figure 3c). Following the series of chalcogenides, a natural choice would be polonium as X ion; since we want to avoid to use unstable elements, another possibility is to partially substitute for the Mo cation. The substituent atom must be chosen so as to induce structural distortions that lower the covalency of the cation structural site, in order to lower the corresponding cophonicity and hence the vibrational frequencies. We are thus oriented toward cations with ionic radii smaller than that of the Mo atom. Moreover, we want to choose a proper dopant concentration and geometric arrangement of the dopant to preserve the stability of the final system. To this aim, we consider the MoS optimized structure, and we substitute a Mo atom with one Ti atom in such a way that, within a single layer, its first neighboring cation shell is formed only by Mo atoms, building the $Mo_3Ti_1S_8$ (Ti:MoS) system with orthorhombic *Cmcm* (SG 63) symmetry (Figure 4). We then fully optimize the geometry[35] and compare the relative properties with those of the unsubstituted MoS system.

The calculated formation energies ΔH_f (Table 1), relative to those of the MoS system, indicate that MoS and Ti:MoS are the most stable compounds among those considered; in particular, the small difference between MoS and Ti:MoS ΔH_f values (0.04 eV) suggests that both compounds have the same probability to be produced, especially in self-assembling tribological mixtures where both MoS_2 and TiS_2 chemical precursors are present. The Mo→Ti substitution produces a significant distortion of the structure (δ = 0.17 Å), due to a local reduction of the M−S bond covalency that decreases from −0.44 to −0.76 eV. Such a local decrease of the covalency produces a global lowering of the cophonicity of the system, that decreases from 8.3 to 5.9 cm^{-1}. The cation substitution also reduces the symmetries of the system, producing the

DOI: 10.1021/acs.inorgchem.5b00431
Inorg. Chem. 2015, 54, 5739−5744

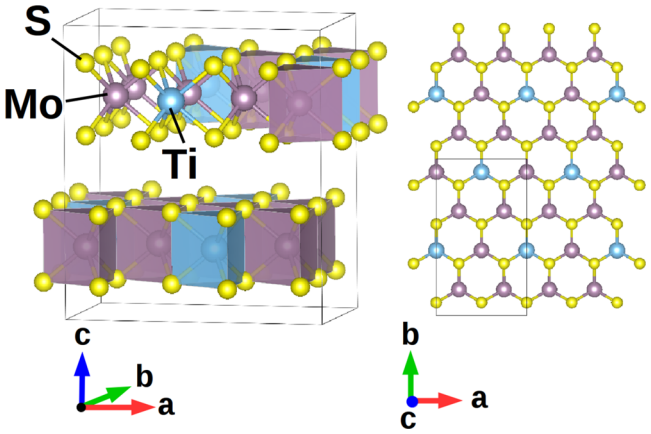

Figure 4. Geometry of the orthorhombic *Cmcm* Ti:MoS_2 model system. Within each layer, one Ti atom is surrounded by only Mo atoms in the first neighboring cation shell.

splitting of those vibrational modes that were degenerate in the parent MoS structure. However, the displacement pattern of those modes that are relevant to the tribological properties is unvaried, and a direct comparison of the corresponding frequencies can be done without ambiguities. In the Ti:MoS system, the vibrational frequencies are found to be lower than those of the undoped counterpart, as expected according to the lower M−S cophonicity (Table 1); in particular, we note that the frequency values are close to those found in the WSe and WTe systems. According to the present results, the bulk contribution to the friction coefficient of the Ti:MoS, WSe, and WTe systems are expected to be similar and the lowest among those of the TMDs compounds considered in this work.

CONCLUSIONS

Six transition metal dichalcogenides with general stoichiometry MX_2 have been studied by means of ab initio techniques. The frequency analysis suggests that the WSe and WTe compounds are expected to display the lowest bulk contribution to the friction coefficient among those of the considered systems. A new lattice dynamic metric, named cophonicity, has been proposed, to capture the effect of the electronic features of the ion environment on the stability of the lattice distortions. We find that cophonicity of the M−X pair in MX_2 TMDs is related to the vibrational frequencies of the distortion modes relevant to the microscopic friction. In particular, we find that, as cophonicity tends to zero, the stability of layer sliding modes is lowered, favoring the relative shift of two subsequent MX_2 layers; in correspondence, a lower macroscopic friction coefficient is expected.

Cophonicity in the studied TMDs is found to be related to the covalency of the M−X bond. Increasing structural distortions in MoX systems induces a lowering of the Mo−X bond covalency, and the Mo−X pair approaches the perfect cophonicity. Following these outcomes, we design the Ti:MoS compound, a new material derived from the MoS_2 TMD by partial Mo→Ti substitution. The analysis of the vibrational frequencies suggests that the Ti:MoS system is expected to have a bulk contribution to the friction coefficient comparable to that of the WSe and WTe compounds.

The cophonicity metric here proposed, combined with electro-structural analyses, constitutes a new tool to finely tune the dynamic properties of a system at the atomic scale; thanks to the generality of its definition, this new lattice dynamic descriptor can be universally applied to any A−B atomic pair, irrespective of the geometric environment in which the pair is embedded.

ASSOCIATED CONTENT

Supporting Information

Covalency metric and the mathematical definition of the cophonicity metric. The Supporting Information is available free of charge on the ACS Publications website at DOI: 10.1021/acs.inorgchem.5b00431.

AUTHOR INFORMATION

Corresponding Author

*E-mail: cammaant@fel.cvut.cz.

Notes

The authors declare no competing financial interest.

ACKNOWLEDGMENTS

This work has been done with the support of intersectoral mobility and quality enhancement of research teams at Czech Technical University in Prague, CZ.1.07/2.3.00/30.0034. This work was supported by the IT4Innovations Centre of Excellence project (CZ.1.05/1.1.00/02.0070), funded by the European Regional Development Fund and the national budget of the Czech Republic via the Research and Development for Innovations Operational Programme, as well as Czech Ministry of Education, Youth and Sports via the project Large Research, Development and Innovations Infrastructures (LM2011033). The use of VESTA[36] software is also acknowledged.

REFERENCES

(1) Pereira, G.; Lachenwitzer, A.; Kasrai, M.; Norton, P.; Capehart, T.; Perry, T.; Cheng, Y.-T.; Frazer, B.; Gilbert, P. *Tribol. Lett.* **2007**, *26*, 103−117.
(2) Vanossi, A.; Manini, N.; Urbakh, M.; Zapperi, S.; Tosatti, E. *Rev. Mod. Phys.* **2013**, *85*, 529−552.
(3) Chhowalla, M.; Shin, H. S.; Eda, G.; Li, L.-J.; Loh, K. P.; Zhang, H. *Nat. Chem.* **2013**, *5*, 263−275.
(4) Wang, Q. H.; Kalantar-Zadeh, K.; Kis, A.; Coleman, J. N.; Strano, M. S. *Nat. Nanotechnol.* **2012**, *7*, 699−712.
(5) Yin, Z.; Li, H.; Li, H.; Jiang, L.; Shi, Y.; Sun, Y.; Lu, G.; Zhang, Q.; Chen, X.; Zhang, H. *ACS Nano* **2012**, *6*, 74−80.
(6) Mak, K. F.; Lee, C.; Hone, J.; Shan, J.; Heinz, T. F. *Phys. Rev. Lett.* **2010**, *105*, 136805.
(7) Cahangirov, S.; Ataca, C.; Topsakal, M.; Sahin, H.; Ciraci, S. *Phys. Rev. Lett.* **2012**, *108*, 126103.
(8) Onodera, T.; Morita, Y.; Suzuki, A.; Koyama, M.; Tsuboi, H.; Hatakeyama, N.; Endou, A.; Takaba, H.; Kubo, M.; Dassenoy, F.; Minfray, C.; Joly-Pottuz, L.; Martin, J.-M.; Miyamoto, A. *J. Phys. Chem. B* **2009**, *113*, 16526−16536.
(9) Onodera, T.; Morita, Y.; Nagumo, R.; Miura, R.; Suzuki, A.; Tsuboi, H.; Hatakeyama, N.; Endou, A.; Takaba, H.; Dassenoy, F.; Minfray, C.; Joly-Pottuz, L.; Kubo, M.; Martin, J.-M.; Miyamoto, A. *J. Phys. Chem. B* **2010**, *114*, 15832.
(10) Liang, T.; Sawyer, W. G.; Perry, S. S.; Sinnott, S. B.; Phillpot, S. R. *Phys. Rev. B* **2008**, *77*, 104105.
(11) Morita, Y.; Onodera, T.; Suzuki, A.; Sahnoun, R.; Koyama, M.; Tsuboi, H.; Hatakeyama, N.; Endou, A.; Takaba, H.; Kubo, M.; Carpio, C. A. D.; Shin-yoshi, T.; Nishino, N.; Suzuki, A.; Miyamoto, A. *Appl. Surf. Sci.* **2008**, *254*, 7618−7621.
(12) Levita, G.; Cavaleiro, A.; Molinari, E.; Polcar, T.; Righi, M. C. *J. Phys. Chem. C* **2014**, *118*, 13809−13816.
(13) Perdew, J. P.; Burke, K.; Ernzerhof, M. *Phys. Rev. Lett.* **1996**, *77*, 3865−3868.

DOI: 10.1021/acs.inorgchem.5b00431
Inorg. Chem. 2015, 54, 5739−5744

(14) (a) Kresse, G.; Furthmüller, J. *Comput. Mater. Sci.* **1996**, *6*, 15−50;(b) Kresse, G.; Joubert, D. *Phys. Rev. B* **1999**, *59*, 1758−1775.
(15) Geim, A. K.; Grigorieva, I. V. *Nature* **2013**, *499*, 419−425.
(16) Grimme, S. *J. Comput. Chem.* **2006**, *27*, 1787−1799.
(17) Schönfeld, B.; Huang, J. J.; Moss, S. C. *Acta Crystallogr., Sect. B* **1983**, *39*, 404−407.
(18) Kalikhman, V. *Inorg. Mater.* **1983**, *19*, 957−962.
(19) Brixner, L. *J. Inorg. Nucl. Chem.* **1962**, *24*, 257−263.
(20) Schutte, W.; Boer, J. D.; Jellinek, F. *J. Solid State Chem.* **1987**, *70*, 207−209.
(21) Kalikhman, V. L. *Neorg. Mater.* **1983**, *19*, 1060−1065.
(22) Yanaki, A. A.; Obolonchik, V. A. *Inorg. Mater.* **1973**, *9*, 1855−1858.
(23) Togo, A.; Oba, F.; Tanaka, I. *Phys. Rev. B* **2008**, *78*, 134106.
(24) Lee, C.; Li, Q.; Kalb, W.; Liu, X.-Z.; Berger, H.; Carpick, R. W.; Hone, J. *Science* **2010**, *328*, 76−80.
(25) Kim, Y.; Huang, J.; Lieber, C. M. *Appl. Phys. Lett.* **1991**, *59*, 3404−3406.
(26) Cao, K.; Li, C.; Yonghua, C.; Tang, H.; Yan, F.; Song, H.; Yang, X. *Tribol. Trans.* **2012**, *55*, 297−301.
(27) Oviedo, J. P.; KC, S.; Lu, N.; Wang, J.; Cho, K.; Wallace, R. M.; Kim, M. J. *ACS Nano* **2015**, *9*, 1543−1551.
(28) Chhowalla, M.; Amaratunga, G. A. J. *Nature* **2000**, *407*, 164−167.
(29) Dominguez-Meister, S.; Justo, A.; Sanchez-Lopez, J. *Mater. Chem. Phys.* **2013**, *142*, 186−194.
(30) Cohen, S.; Rapoport, L.; Ponomarev, E.; Cohen, H.; Tsirlina, T.; Tenne, R.; Lévy-Clément, C. *Thin Solid Films* **1998**, *324*, 190−197.
(31) The geometric distortion δ is defined as

$$\delta = \sqrt{\frac{A_s}{A_p} \sum_{i,j} (r_{i,j} - x_{i,j})^2} \quad (1)$$

where A_p and A_s are the volume of the parent and distorted structure, respectively, while $r_{i,j}$ and $x_{i,j}$ are the j-th Cartesian components of the i-th atom of the parent and distorted structure, respectively. Distorted structures are from the corresponding ones in the parent phase. The complete mathematical derivation is described in ref 32.
(32) Campbell, B. J.; Stokes, H. T.; Tanner, D. E.; Hatch, D. M. *J. Appl. Crystallogr.* **2006**, *39*, 607−614.
(33) Cammarata, A.; Rondinelli, J. M. *J. Chem. Phys.* **2014**, *141*, 114704.
(34) Parlinski, K.; Li, Z. Q.; Kawazoe, Y. *Phys. Rev. Lett.* **1997**, *78*, 4063−4066.
(35) Optimized parameters of the orthorhombic *Cmcm* Ti:MoS model are the following: (i) lattice parameters (Å), a = 6.463 21, b = 11.194 61, c = 12.567 47; (ii) Wyckoff positions, Mo 4c (0, −0.082 43, ($^1/_4$)), Ti 4c (0, 0.417 44, ($^1/_4$)) Mo 8g (($^1/_4$), 0.167 67, ($^1/_4$)), S 8f (0, 0.584 87, 0.128 45), S 8f (0, 0.084 24, 0.126 85), S 16h (0.748 66, 0.333 85, 0.128 31).
(36) Momma, K.; Izumi, F. *J. Appl. Crystallogr.* **2008**, *41*, 653−658.

DOI: 10.1021/acs.inorgchem.5b00431
Inorg. Chem. 2015, 54, 5739−5744